

**Production of ω mesons at Large Transverse Momenta
in $p + p$ and $d + \text{Au}$ Collisions at $\sqrt{s_{NN}} = 200 \text{ GeV}$**

S.S. Adler,⁵ S. Afanasiev,²⁰ C. Aidala,¹⁰ N.N. Ajitanand,⁴⁴ Y. Akiba,^{21,40} A. Al-Jamel,³⁵ J. Alexander,⁴⁴ K. Aoki,²⁵ L. Aphecetche,⁴⁶ R. Armendariz,³⁵ S.H. Aronson,⁵ R. Averbeck,⁴⁵ T.C. Awes,³⁶ V. Babintsev,¹⁷ A. Baldisseri,¹¹ K.N. Barish,⁶ P.D. Barnes,²⁸ B. Bassalleck,³⁴ S. Bathe,^{6,31} S. Batsouli,¹⁰ V. Baublis,³⁹ F. Bauer,⁶ A. Bazilevsky,^{5,41} S. Belikov,^{19,17} M.T. Bjornndal,¹⁰ J.G. Boissevain,²⁸ H. Borel,¹¹ M.L. Brooks,²⁸ D.S. Brown,³⁵ N. Bruner,³⁴ D. Bucher,³¹ H. Buesching,^{5,31} V. Bumazhnov,¹⁷ G. Bunce,^{5,41} J.M. Burward-Hoy,^{28,27} S. Butsyk,⁴⁵ X. Camard,⁴⁶ P. Chand,⁴ W.C. Chang,² S. Chernichenko,¹⁷ C.Y. Chi,¹⁰ J. Chiba,²¹ M. Chiu,¹⁰ I.J. Choi,⁵³ R.K. Choudhury,⁴ T. Chujo,⁵ V. Cianciolo,³⁶ Y. Cobigo,¹¹ B.A. Cole,¹⁰ M.P. Comets,³⁷ P. Constantin,¹⁹ M. Csanád,¹³ T. Csörgő,²² J.P. Cussonneau,⁴⁶ D. d'Enterria,¹⁰ K. Das,¹⁴ G. David,⁵ F. Deák,¹³ H. Delagrangé,⁴⁶ A. Denisov,¹⁷ A. Deshpande,⁴¹ E.J. Desmond,⁵ A. Devismes,⁴⁵ O. Dietzsch,⁴² J.L. Drachenberg,¹ O. Drapier,²⁶ A. Drees,⁴⁵ A. Durum,¹⁷ D. Dutta,⁴ V. Dzhordzhadze,⁴⁷ Y.V. Efremenko,³⁶ H. En'yo,^{40,41} B. Espagnon,³⁷ S. Esumi,⁴⁹ D.E. Fields,^{34,41} C. Finck,⁴⁶ F. Fleuret,²⁶ S.L. Fokin,²⁴ B.D. Fox,⁴¹ Z. Fraenkel,⁵² J.E. Frantz,¹⁰ A. Franz,⁵ A.D. Frawley,¹⁴ Y. Fukao,^{25,40,41} S.-Y. Fung,⁶ S. Gadrat,²⁹ M. Germain,⁴⁶ A. Glenn,⁴⁷ M. Gonin,²⁶ J. Gosset,¹¹ Y. Goto,^{40,41} R. Granier de Cassagnac,²⁶ N. Grau,¹⁹ S.V. Greene,⁵⁰ M. Grosse Perdekamp,^{18,41} H.-Å. Gustafsson,³⁰ T. Hachiya,¹⁶ J.S. Haggerty,⁵ H. Hamagaki,⁸ A.G. Hansen,²⁸ E.P. Hartouni,²⁷ M. Harvey,⁵ K. Hasuko,⁴⁰ R. Hayano,⁸ X. He,¹⁵ M. Heffner,²⁷ T.K. Hemmick,⁴⁵ J.M. Heuser,⁴⁰ P. Hidas,²² H. Hiejima,¹⁸ J.C. Hill,¹⁹ R. Hobbs,³⁴ W. Holzmann,⁴⁴ K. Homma,¹⁶ B. Hong,²³ A. Hoover,³⁵ T. Horaguchi,^{40,41,48} T. Ichihara,^{40,41} V.V. Ikonnikov,²⁴ K. Imai,^{25,40} M. Inaba,⁴⁹ M. Inuzuka,⁸ D. Isenhower,¹ L. Isenhower,¹ M. Ishihara,⁴⁰ M. Issah,⁴⁴ A. Isupov,²⁰ B.V. Jacak,⁴⁵ J. Jia,⁴⁵ O. Jinnouchi,^{40,41} B.M. Johnson,⁵ S.C. Johnson,²⁷ K.S. Joo,³² D. Jouan,³⁷ F. Kajihara,⁸ S. Kametani,^{8,51} N. Kamihara,^{40,48} M. Kaneta,⁴¹ J.H. Kang,⁵³ K. Katou,⁵¹ T. Kawabata,⁸ A.V. Kazantsev,²⁴ S. Kelly,^{9,10} B. Khachaturov,⁵² A. Khanzadeev,³⁹ J. Kikuchi,⁵¹ D.J. Kim,⁵³ E. Kim,⁴³ G.-B. Kim,²⁶ H.J. Kim,⁵³ E. Kinney,⁹ A. Kiss,¹³ E. Kistenev,⁵ A. Kiyomichi,⁴⁰ C. Klein-Boesing,³¹ H. Kobayashi,⁴¹ L. Kochenda,³⁹ V. Kochetkov,¹⁷ R. Kohara,¹⁶ B. Komkov,³⁹ M. Konno,⁴⁹ D. Kotchetkov,⁶ A. Kozlov,⁵² P.J. Kroon,⁵ C.H. Kuberg,^{1,*} G.J. Kunde,²⁸ K. Kurita,⁴⁰ M.J. Kweon,²³ Y. Kwon,⁵³ G.S. Kyle,³⁵ R. Lacey,⁴⁴ J.G. Lajoie,¹⁹ Y. Le Bornec,³⁷ A. Lebedev,^{19,24} S. Leckey,⁴⁵ D.M. Lee,²⁸ M.J. Leitch,²⁸ M.A.L. Leite,⁴² X.H. Li,⁶ H. Lim,⁴³ A. Litvinenko,²⁰ M.X. Liu,²⁸ C.F. Maguire,⁵⁰ Y.I. Makdisi,⁵ A. Malakhov,²⁰ V.I. Manko,²⁴ Y. Mao,^{38,40} G. Martinez,⁴⁶ H. Masui,⁴⁹ F. Matathias,⁴⁵ T. Matsumoto,^{8,51} M.C. McCain,¹ P.L. McGaughey,²⁸ Y. Miake,⁴⁹ T.E. Miller,⁵⁰ A. Milov,⁴⁵ S. Mioduszewski,⁵ G.C. Mishra,¹⁵ J.T. Mitchell,⁵ A.K. Mohanty,⁴ D.P. Morrison,⁵ J.M. Moss,²⁸ D. Mukhopadhyay,⁵² M. Muniruzzaman,⁶ S. Nagamiya,²¹ J.L. Nagle,^{9,10} T. Nakamura,¹⁶ J. Newby,⁴⁷ A.S. Nyanin,²⁴ J. Nystrand,³⁰ E. O'Brien,⁵ C.A. Ogilvie,¹⁹ H. Ohnishi,⁴⁰ I.D. Ojha,^{3,50} H. Okada,^{25,40} K. Okada,^{40,41} A. Oskarsson,³⁰ I. Otterlund,³⁰ K. Oyama,⁸ K. Ozawa,⁸ D. Pal,⁵² A.P.T. Palounek,²⁸ V. Pantuev,⁴⁵ V. Papavassiliou,³⁵ J. Park,⁴³ W.J. Park,²³ S.F. Pate,³⁵ H. Pei,¹⁹ V. Penev,²⁰ J.-C. Peng,¹⁸ H. Pereira,¹¹ V. Peresedov,²⁰ A. Pierson,³⁴ C. Pinkenburg,⁵ R.P. Pisani,⁵ M.L. Purschke,⁵ A.K. Purwar,⁴⁵ J.M. Qualls,¹ J. Rak,¹⁹ I. Ravinovich,⁵² K.F. Read,^{36,47} M. Reuter,⁴⁵ K. Reygers,³¹ V. Riabov,³⁹ Y. Riabov,³⁹ G. Roche,²⁹ A. Romana,^{26,*} M. Rosati,¹⁹ S.S.E. Rosendahl,³⁰ P. Rosnet,²⁹ V.L. Rykov,⁴⁰ S.S. Ryu,⁵³ N. Saito,^{25,40,41} T. Sakaguchi,^{8,51} S. Sakai,⁴⁹ V. Samsonov,³⁹ L. Sanfratello,³⁴ R. Santo,³¹ H.D. Sato,^{25,40} S. Sato,^{5,49} S. Sawada,²¹ Y. Schutz,⁴⁶ V. Semenov,¹⁷ R. Seto,⁶ T.K. Shea,⁵ I. Shein,¹⁷ T.-A. Shibata,^{40,48} K. Shigaki,¹⁶ M. Shimomura,⁴⁹ A. Sickles,⁴⁵ C.L. Silva,⁴² D. Silvermyr,²⁸ K.S. Sim,²³ A. Soldatov,¹⁷ R.A. Soltz,²⁷ W.E. Sondheim,²⁸ S.P. Sorensen,⁴⁷ I.V. Sourikova,⁵ F. Staley,¹¹ P.W. Stankus,³⁶ E. Stenlund,³⁰ M. Stepanov,³⁵ A. Ster,²² S.P. Stoll,⁵ T. Sugitate,¹⁶ J.P. Sullivan,²⁸ S. Takagi,⁴⁹ E.M. Takagui,⁴² A. Taketani,^{40,41} K.H. Tanaka,²¹ Y. Tanaka,³³ K. Tanida,⁴⁰ M.J. Tannenbaum,⁵ A. Taranenko,⁴⁴ P. Tarján,¹² T.L. Thomas,³⁴ M. Togawa,^{25,40} J. Tojo,⁴⁰ H. Torii,^{25,41} R.S. Towell,¹ V.-N. Tram,²⁶ I. Tserruya,⁵² Y. Tsuchimoto,¹⁶ H. Tydesjö,³⁰ N. Tyurin,¹⁷ T.J. Uam,³² J. Velkovska,⁵ M. Velkovsky,⁴⁵ V. Veszprémi,¹² A.A. Vinogradov,²⁴ M.A. Volkov,²⁴ E. Vznuzdaev,³⁹ X.R. Wang,¹⁵ Y. Watanabe,^{40,41} S.N. White,⁵ N. Willis,³⁷ F.K. Wohn,¹⁹ C.L. Woody,⁵ W. Xie,⁶ A. Yanovich,¹⁷ S. Yokkaichi,^{40,41} G.R. Young,³⁶ I.E. Yushmanov,²⁴ W.A. Zajc,^{10,†} C. Zhang,¹⁰ S. Zhou,⁷ J. Zimányi,^{22,*} L. Zolin,²⁰ X. Zong,¹⁹ and H.W. vanHecke²⁸

(PHENIX Collaboration)

¹Abilene Christian University, Abilene, TX 79699, USA

²Institute of Physics, Academia Sinica, Taipei 11529, Taiwan

³Department of Physics, Banaras Hindu University, Varanasi 221005, India

- ⁴Bhabha Atomic Research Centre, Bombay 400 085, India
⁵Brookhaven National Laboratory, Upton, NY 11973-5000, USA
⁶University of California - Riverside, Riverside, CA 92521, USA
⁷China Institute of Atomic Energy (CIAE), Beijing, People's Republic of China
⁸Center for Nuclear Study, Graduate School of Science, University of Tokyo, 7-3-1 Hongo, Bunkyo, Tokyo 113-0033, Japan
⁹University of Colorado, Boulder, CO 80309, USA
¹⁰Columbia University, New York, NY 10027 and Nevis Laboratories, Irvington, NY 10533, USA
¹¹Dapnia, CEA Saclay, F-91191, Gif-sur-Yvette, France
¹²Debrecen University, H-4010 Debrecen, Egyetem tér 1, Hungary
¹³ELTE, Eötvös Loránd University, H - 1117 Budapest, Pázmány P. s. 1/A, Hungary
¹⁴Florida State University, Tallahassee, FL 32306, USA
¹⁵Georgia State University, Atlanta, GA 30303, USA
¹⁶Hiroshima University, Kagamiyama, Higashi-Hiroshima 739-8526, Japan
¹⁷IHEP Protvino, State Research Center of Russian Federation, Institute for High Energy Physics, Protvino, 142281, Russia
¹⁸University of Illinois at Urbana-Champaign, Urbana, IL 61801, USA
¹⁹Iowa State University, Ames, IA 50011, USA
²⁰Joint Institute for Nuclear Research, 141980 Dubna, Moscow Region, Russia
²¹KEK, High Energy Accelerator Research Organization, Tsukuba, Ibaraki 305-0801, Japan
²²KFKI Research Institute for Particle and Nuclear Physics of the Hungarian Academy of Sciences (MTA KFKI RMKI), H-1525 Budapest 114, POBox 49, Budapest, Hungary
²³Korea University, Seoul, 136-701, Korea
²⁴Russian Research Center "Kurchatov Institute", Moscow, Russia
²⁵Kyoto University, Kyoto 606-8502, Japan
²⁶Laboratoire Leprince-Ringuet, Ecole Polytechnique, CNRS-IN2P3, Route de Saclay, F-91128, Palaiseau, France
²⁷Lawrence Livermore National Laboratory, Livermore, CA 94550, USA
²⁸Los Alamos National Laboratory, Los Alamos, NM 87545, USA
²⁹LPC, Université Blaise Pascal, CNRS-IN2P3, Clermont-Fd, 63177 Aubiere Cedex, France
³⁰Department of Physics, Lund University, Box 118, SE-221 00 Lund, Sweden
³¹Institut für Kernphysik, University of Muenster, D-48149 Muenster, Germany
³²Myongji University, Yongin, Kyonggido 449-728, Korea
³³Nagasaki Institute of Applied Science, Nagasaki-shi, Nagasaki 851-0193, Japan
³⁴University of New Mexico, Albuquerque, NM 87131, USA
³⁵New Mexico State University, Las Cruces, NM 88003, USA
³⁶Oak Ridge National Laboratory, Oak Ridge, TN 37831, USA
³⁷IPN-Orsay, Université Paris Sud, CNRS-IN2P3, BP1, F-91406, Orsay, France
³⁸Peking University, Beijing, People's Republic of China
³⁹PNPI, Petersburg Nuclear Physics Institute, Gatchina, Leningrad region, 188300, Russia
⁴⁰RIKEN (The Institute of Physical and Chemical Research), Wako, Saitama 351-0198, JAPAN
⁴¹RIKEN BNL Research Center, Brookhaven National Laboratory, Upton, NY 11973-5000, USA
⁴²Universidade de São Paulo, Instituto de Física, Caixa Postal 66318, São Paulo CEP05315-970, Brazil
⁴³System Electronics Laboratory, Seoul National University, Seoul, South Korea
⁴⁴Chemistry Department, Stony Brook University, Stony Brook, SUNY, NY 11794-3400, USA
⁴⁵Department of Physics and Astronomy, Stony Brook University, SUNY, Stony Brook, NY 11794, USA
⁴⁶SUBATECH (Ecole des Mines de Nantes, CNRS-IN2P3, Université de Nantes) BP 20722 - 44307, Nantes, France
⁴⁷University of Tennessee, Knoxville, TN 37996, USA
⁴⁸Department of Physics, Tokyo Institute of Technology, Oh-okayama, Meguro, Tokyo 152-8551, Japan
⁴⁹Institute of Physics, University of Tsukuba, Tsukuba, Ibaraki 305, Japan
⁵⁰Vanderbilt University, Nashville, TN 37235, USA
⁵¹Waseda University, Advanced Research Institute for Science and Engineering, 17 Kikui-cho, Shinjuku-ku, Tokyo 162-0044, Japan
⁵²Weizmann Institute, Rehovot 76100, Israel
⁵³Yonsei University, IPAP, Seoul 120-749, Korea

(Dated: September 17, 2018)

The PHENIX experiment at RHIC has measured the invariant cross section for ω -meson production at mid-rapidity in the transverse momentum range $2.5 < p_T < 9.25$ GeV/c in $p + p$ and $d+Au$ collisions at $\sqrt{s_{NN}} = 200$ GeV. Measurements in two decay channels ($\omega \rightarrow \pi^0 \pi^+ \pi^-$ and $\omega \rightarrow \pi^0 \gamma$) yield consistent results, and the reconstructed ω mass agrees with the accepted value within the p_T range of the measurements. The ω/π^0 ratio is found to be $0.85 \pm 0.05^{\text{stat}} \pm 0.09^{\text{sys}}$ in $p + p$ and $0.94 \pm 0.08^{\text{stat}} \pm 0.12^{\text{sys}}$ in $d+Au$ collisions, independent of p_T . The nuclear modification factor R_{dA}^{ω} is $1.03 \pm 0.12^{\text{stat}} \pm 0.21^{\text{sys}}$ and $0.83 \pm 0.21^{\text{stat}} \pm 0.17^{\text{sys}}$ in minimum bias and central (0-20%) $d+Au$ collisions, respectively.

Cross sections at large transverse momentum (p_T) for products of “hard” point-like processes (*e.g.*, inclusive hadrons, jets, direct γ 's, and heavy flavor) in high energy hadron collisions are well described in perturbative Quantum Chromodynamics (pQCD) [1]. As a result they are considered to be well-calibrated probes of small-distance QCD phenomena. When going from $p+p$ to $p(\text{or } d)+A$ and $A+A$ collisions, deviations from cross section scaling with respect to the number of binary $N+N$ collisions provide information on cold nuclear matter effects such as initial state energy loss [2], shadowing [3] and hot nuclear matter effects such as in-medium energy loss [4], increasing importance of production via recombination [5], and modifications to the QCD vacuum [6].

Production of ω mesons at high- p_T is especially interesting. The ω and π^0 are vector and pseudoscalar mesons, respectively. The ω/π^0 ratio carries information about probabilities of corresponding spin states to be produced in hadronization. Furthermore, ω mesons can be used as a probe of the nuclear medium since a significant fraction of them produced in $A+A$ or $p(d)+A$ collisions will decay inside the produced medium ($c\tau = 23.8$ fm) possibly leading to changes of the mass and/or width of the ω with respect to their values in vacuum.

The PHENIX [7] experiment at RHIC has a unique capability to measure both neutral and charged products of $A+A$ and $p+p$ collisions at very high event rates. The two central arm spectrometers each cover 90° in azimuth and ± 0.35 in pseudorapidity. The Electromagnetic Calorimeter (EMCal), with energy resolution $\sigma/E = 8.1\%/\sqrt{E(\text{GeV})} \oplus 2.1\%$, is used to reconstruct γ 's and π^0 's. For charged particle reconstruction two layers of Pad Chambers provide 3D pattern recognition and fake track rejection, and a Drift Chamber gives momentum resolution $\sigma/p_T = 0.7\%\sqrt{p_T(\text{GeV}/c)} \oplus 1.1\%$. Beam-Beam counters (BBC) were used to provide minimum bias trigger and to determine the collision vertex. The minimum bias trigger cross sections measured by the BBC are 23.0 ± 2.2 mb in $p+p$ [8] and 1.99 ± 0.10 b in $d+Au$ [9] collisions. In $d+Au$ collisions the BBC were also used to separate events into centrality classes as explained in [10]. High p_T online triggers are implemented by adding together amplitudes in 4×4 adjacent EMCal towers and comparing them to a threshold of 1.4 GeV in $p+p$ and 2.4 GeV in $d+Au$. The trigger could be fired by one or more photons coming from ω decay final states including 3γ or $2\pi 2\gamma$.

The data was collected by the PHENIX experiment during RHIC Run3. After selecting good runs and cutting on the collision vertex ($|z| < 30$ cm) we analyzed approximately 4.6×10^7 and 2.1×10^7 high p_T trigger events, corresponding to a total integrated luminosity of 0.22 pb^{-1} and 1.5 nb^{-1} in the $p+p$ and $d+Au$ collision systems, respectively.

Although ω -mesons are relatively abundant in high energy hadronic collisions ($\omega/\pi^0 \approx 1$ at high p_T), their

measurement is challenging due to the multi-particle final states of the main decay channels and the combinatorial background associated with their reconstruction.

The procedure used to measure $\omega \rightarrow \pi^0\pi^+\pi^-$ is the same as used to measure $\eta \rightarrow \pi^0\pi^+\pi^-$ [10]. In case of ω one shall account for a wider peak and different phase space density of the 3-body decay [11, 12]. The analysis procedure for the photonic decay mode, $\omega \rightarrow \pi^0\gamma \rightarrow 3\gamma$, is very similar to earlier PHENIX measurements of other mesons with photonic decay modes, $\pi^0, \eta \rightarrow 2\gamma$ [8, 13, 14]. For both ω decay modes studied the first step is to reconstruct π^0 candidates by combining photon pairs and applying a p_T dependent cut around the mass of the π^0 . The R.M.S. of the π^0 peak varies with p_T from 8 MeV to 13 MeV. Candidates (which include combinatorial background) are combined with a third photon for $\omega \rightarrow \pi^0\gamma$ or with two unidentified charged tracks (assumed to be π -mesons) for $\omega \rightarrow \pi^0\pi^+\pi^-$. Raw yields are extracted by fitting the p_T slices of the invariant mass distribution as in the insert panel in Fig. 1. The signal to background ratio (S/B) of $\pi^0\pi^+\pi^-$ decay channel is 1:7 at low p_T and grows to 1:1 with p_T in $p+p$ collisions. In $d+Au$ collisions it starts at 1:20 and grows with p_T to 1:2. For the $\pi^0\gamma$ channel S/B is 1.5-2 times worse. Corrections for acceptance, trigger efficiency, and analysis cuts are described in detail in [10]. Further details about the analysis procedures can be found in [15].

We classify systematic error sources as type A (point-to-point uncorrelated, which can move each point independently), type B (point-to-point correlated, which can move points coherently, but potentially by different relative amounts), and type C (global, which move all points by the same relative amount). These errors are summarized in Table I for the different decay modes and collision systems. Major contributors include signal extraction (type A), online high- p_T trigger efficiency (type B) and the total cross-section measurement (type C). The uncertainty on the signal extraction, which is the dominant source of systematic error, is relatively large due to the fact that correlations in the triggered sample rendered background subtraction via event mixing impossible, and therefore the unknown shape of the underlying background had to be accounted for in the peak fit. This error is estimated based on variation of analysis cuts and fitting procedures [10].

Figure 1 shows the invariant cross sections for ω production in $p+p$, minimum bias $d+Au$, and central (0-20%) $d+Au$ collisions at $\sqrt{s_{NN}} = 200$ GeV, as a function of p_T . The p_T range ($2.5 < p_T < 9.25$ GeV/ c) is limited by statistics at high p_T , and by decreasing detector acceptance and trigger efficiency at low p_T . The results for the two decay modes, which involve different kinematics, detector acceptance, and efficiency corrections, agree very well.

Figure 2 shows the results for the ratio of vector to pseudoscalar meson production (ω/π^0) in $d+Au$ and $p+p$

TABLE I: Systematic errors for the ω production cross section for the two decay channels and the two collision systems analyzed. Error types are described in the text. Values with a range indicate variation of the systematic error over the p_T range of the measurement.

| Type | $\omega \rightarrow \pi^0 \pi^+ \pi^-$ | | $\omega \rightarrow \pi^0 \gamma$ | |
|------|--|--------|-----------------------------------|---------|
| | $p+p$ | $d+Au$ | $p+p$ | $d+Au$ |
| A | 7-20% | 10-15% | 25-40% | 10% |
| B | 8-10% | 11-14% | 5.8-9.2% | 7.4-11% |
| C | 11% | 9.4% | 13% | 11% |

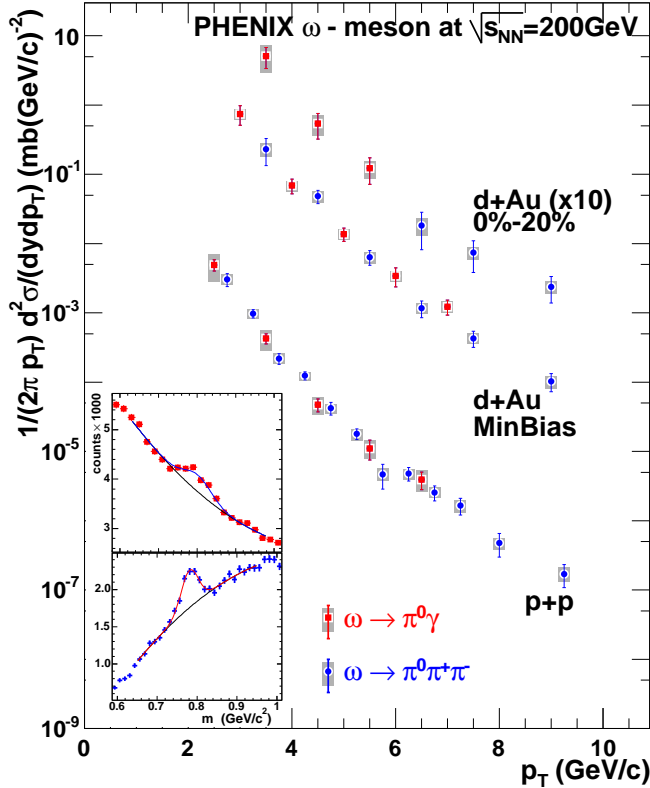


FIG. 1: Invariant cross section of ω production in $p+p$ and $d+Au$ collisions at $\sqrt{s_{NN}} = 200$ GeV measured in $\omega \rightarrow \pi^0 \pi^+ \pi^-$ and $\omega \rightarrow \pi^0 \gamma$ decay channels. Bars and boxes represent statistical and systematic errors, respectively. Fits to invariant mass distributions of $\pi^0 \gamma$ (top) and $\pi^0 \pi^+ \pi^-$ (bottom) are shown in the insert.

p collisions at $\sqrt{s_{NN}} = 200$ GeV. For the denominator we use inclusive π^0 yields measured by PHENIX [8, 16]. Ratios in both systems are consistent with unity over all measured p_T . Fits to a constant yield $\omega/\pi^0 = 0.85 \pm 0.05^{\text{stat}} \pm 0.09^{\text{sys}}$ and $0.94 \pm 0.08^{\text{stat}} \pm 0.12^{\text{sys}}$ in $p+p$ and $d+Au$ collisions, respectively. Fits assuming linear p_T dependence have slopes consistent with zero. At high p_T the PYTHIA [17] prediction for this ratio in $p+p$ collisions at $\sqrt{s} = 200$ GeV is consistent with, but slightly higher than, the measurement.

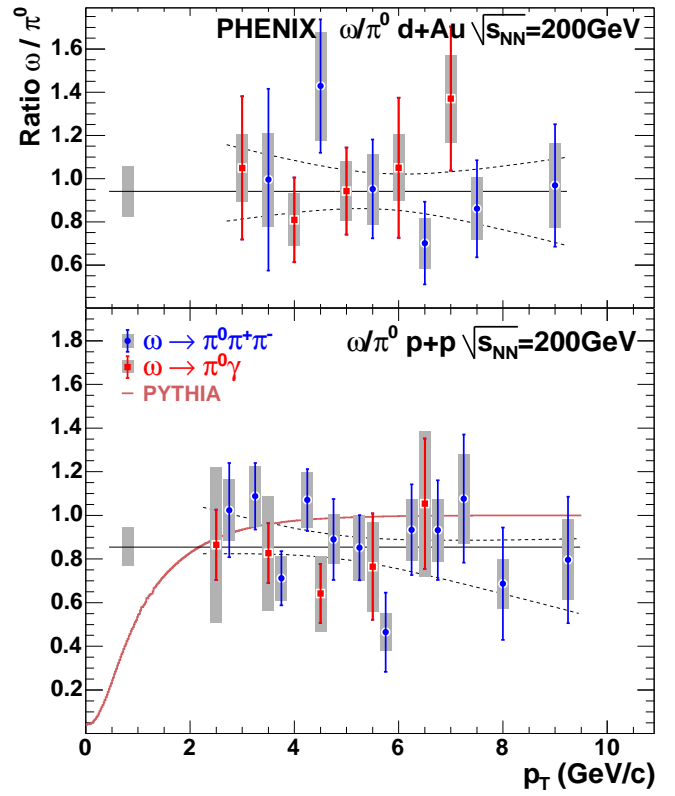


FIG. 2: Measured ω/π^0 vs p_T in (upper panel) $d+Au$ and (lower panel) $p+p$ collisions at $\sqrt{s_{NN}} = 200$ GeV. Straight lines show fits to a constant for each collision system. The boxes at the left edge of the constant fit lines show the systematic error on the data averaged over p_T . Dashed lines show values within 1σ of the best linear fits to the data. The PYTHIA prediction [17] for $p+p$ collisions at $\sqrt{s} = 200$ GeV is shown with a solid curve in the bottom panel.

The R-806 experiment at ISR measured ω/π^0 in $p+p$ collisions at $\sqrt{s} = 62$ GeV [18] and found this ratio to be 0.87 ± 0.17 over $3.5 < p_T < 7$ GeV/c. The E706 experiment measured ω/π^0 in $\pi^- + \text{Be}$ collisions at $\sqrt{s_{\pi N}} = 31$ GeV [19] and found values consistent with the results presented in this paper. The ω/π^0 ratios measured in hadronic interactions by three experiments at three different energies between 31 and 200 GeV, are the same within the errors.

Several LEP experiments [20, 21, 22] have measured ω production in $e^+ + e^-$ collisions at $\sqrt{s} = 91.2$ GeV and presented results as a function of $x_p = 2p_\omega/\sqrt{s}$. This is not a well-defined quantity in hadronic interactions. However, one can compare the ω/π^0 ratio at large values of p_T and x_p . Following the procedure for handling LEP data described in [10] one finds that for $x_p > 0.5$, the largest value for which statistically significant LEP data is available, the ratio has grown to approximately 0.7, close to the measurements in hadronic interactions.

Figure 3 shows the nuclear modification factor R_{dA}^ω , defined as the ratio of the ω meson yields in $d+Au$ in-

interactions and $p + p$ interactions scaled by the number of binary collisions in $d+Au$, for minimum bias and central (0-20%) $d+Au$ events. Precise definition of the R_{dA} and procedure to determine centrality in $d+Au$ is given in sections IV.B and III.C in [10]. We find R_{dA}^ω to be $1.03 \pm 0.12^{\text{stat}} \pm 0.21^{\text{sys}}$ for minimum bias and $0.83 \pm 0.21^{\text{stat}} \pm 0.17^{\text{sys}}$ for central events, independent of p_T . The R_{dA} for two other neutral mesons (π^0 and η) measured by PHENIX [10, 16] are also shown in Fig. 3. In all cases PHENIX observes that R_{dA} is close to one for $p_T > 2 \text{ GeV}/c$ and flat out to the highest p_T . Similar behavior is seen in preliminary analysis of K and ϕ mesons [15, 23].

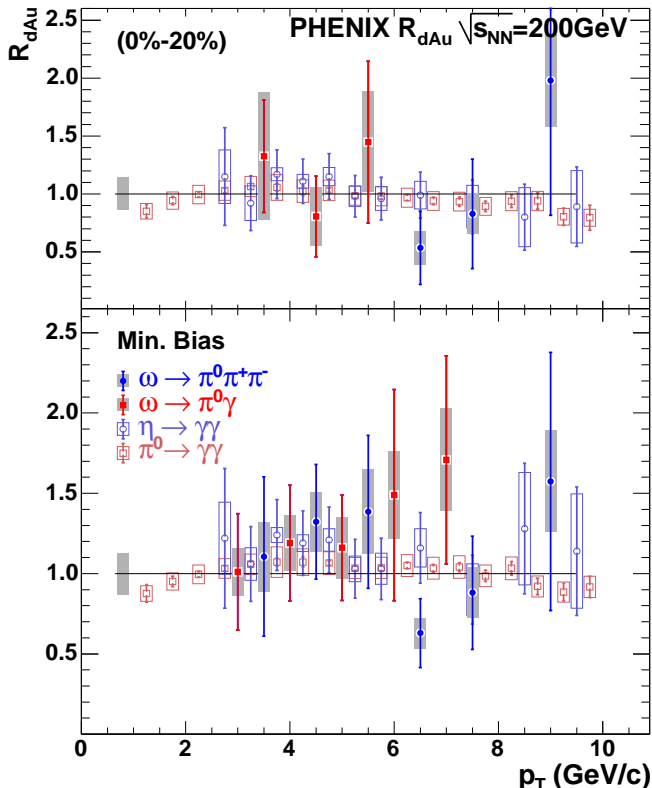


FIG. 3: Measured R_{dA} vs p_T for neutral mesons in $d+Au$ collisions at $\sqrt{s_{NN}} = 200 \text{ GeV}$ for (upper panel) 0%-20% central and (lower panel) minimum bias. Values for π^0 's and η 's are from [10, 16]. For reference a line is plotted at $R_{dA}=1$. The scaling systematic error is shown as a box on the left.

Recent publications suggest that modifications to the ω mass can be observed even in cold matter by studying not only the electron decay channel [24, 25], but also hadronic channels [26]. For the hadronic decay modes presented here PHENIX lacks acceptance at low p_T where the effect is expected to be the most prominent. However, we do have excellent mass resolution (20-25 MeV) for the mixed neutral-charged particle decay mode. Figure 4 shows extracted values for the ω mass as a function of p_T . In the p_T range of the measurement we observe no modification

of the ω mass in either $d+Au$ or $p + p$ collision systems at $\sqrt{s_{NN}} = 200 \text{ GeV}$.

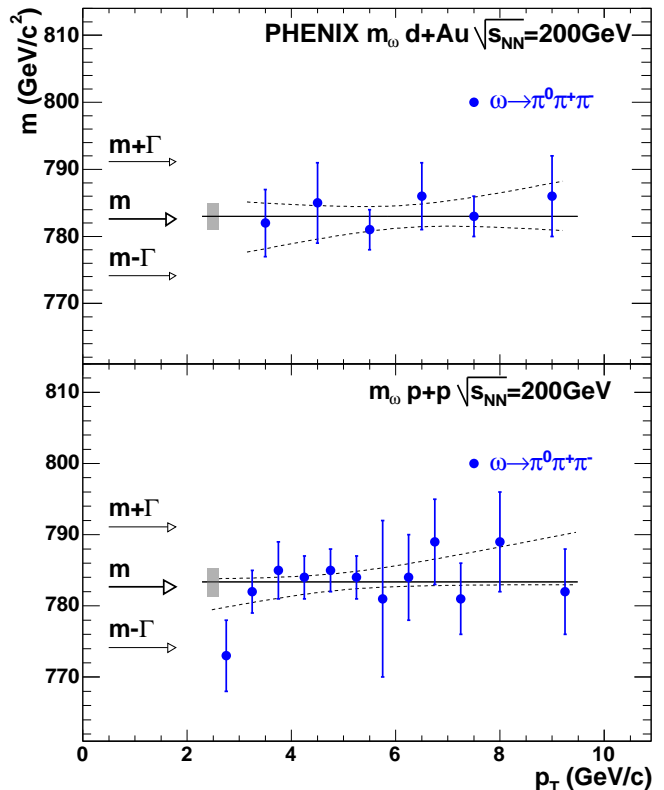


FIG. 4: Reconstructed ω mass measured in the $\pi^0\pi^+\pi^-$ decay channel vs p_T in (upper panel) $d+Au$ and (lower panel) $p + p$ collisions at $\sqrt{s_{NN}} = 200 \text{ GeV}$. Error bars show statistical errors. Straight lines show fits of the data to a constant. Dashed lines show values within 1σ of the best linear fit to the data. Systematic error on the fit value is shown with the box. PDG values for ω meson mass (m) and width (Γ) are shown with arrows on the left [27].

In summary we have presented the first measurement of ω production in $p + p$ and $d+Au$ collisions at $\sqrt{s_{NN}} = 200 \text{ GeV}$. The production cross section is measured in two different decay modes with consistent results. The ω/π^0 ratio in $p + p$ collisions is found to be $0.85 \pm 0.05^{\text{stat}} \pm 0.09^{\text{sys}}$ and $0.94 \pm 0.08^{\text{stat}} \pm 0.12^{\text{sys}}$ in $d+Au$ over the measured p_T range. This agrees with previous measurements in hadronic collisions at lower \sqrt{s} . The nuclear modification factor for ω production in $d+Au$ collisions is consistent with 1 and p_T independent for $p_T > 2 \text{ GeV}/c$ consistent with other meson measurements. No modifications to the ω mass were observed in $p + p$ or $d+Au$ collisions. The ω meson is also interesting as a probe of the hot nuclear medium created in A+A collisions. This measurement will serve as an excellent baseline for measurements of ω production in A+A in various decay channels.

We thank the staff of the Collider-Accelerator and Physics Departments at BNL for their vital contri-

butions. We acknowledge support from the Department of Energy and NSF (U.S.A.), MEXT and JSPS (Japan), CNPq and FAPESP (Brazil), NSFC (China), IN2P3/CNRS, CEA, and ARMINES (France), BMBF, DAAD, and AvH (Germany), OTKA (Hungary), DAE and DST (India), ISF (Israel), KRF and KOSEF (Korea), RMIST, RAS, and RMAE (Russia), VR and KAW (Sweden), U.S. CRDF for the FSU, US-Hungarian NSF-OTKA-MTA, and US-Israel BSF.

* Deceased

† PHENIX Spokesperson: zajc@nevis.columbia.edu

- [1] J.F. Owens, Rev. Mod. Phys. **59**, 465 (1987)
- [2] I. Vitev, Phys. Lett. **B562**, 36 (2003)
- [3] V. Guzey, M. Strikman, W. Vogelsang Phys. Lett. **B603**, 173 (2004)
- [4] R. Baier, D. Schiff and B. Zakharov, Ann. Rev. Nucl. Part. Sci. **50**, 37 (2000)
- [5] R. J. Fries, J. Phys. **G30**, S853 (2004)
- [6] R. Rapp and J. Wambach, Adv. Nucl. Phys. **25**, 1 (2000)
- [7] K. Adcox et al, (PHENIX Collaboration) Nucl. Instrum. Meth. **A499**, 469 (2003)
- [8] S.S. Adler et al, (PHENIX Collaboration) Phys. Rev. Lett. **91**, 182301, (2003)
- [9] S. White, AIP Conf. Proc. **792**, 527 (2005)
- [10] S.S. Adler et al, (PHENIX Collaboration) nucl-ex/0611006
- [11] C. Alff et al, Phys. Rev. Lett. **9** 325 (1962)
- [12] M.L. Stevenson, Phys. Rev. **125**, 687 (1962)
- [13] S.S. Adler et al, (PHENIX Collaboration) Phys. Rev. Lett. **91**, 072301, (2003)
- [14] S.S. Adler et al, (PHENIX Collaboration) Phys. Rev. Lett. **96**, 202301, (2006)
- [15] V. Riabov (for the PHENIX Collaboration) Nucl. Phys. **A774**, 735-738, (2006)
- [16] S.S. Adler et al, (PHENIX Collaboration) Phys. Rev. Lett. **91**, 072303, (2003)
- [17] PYTHIA 6.206, T. Sjostrand et al, hep-ph/0108264 used with default parameters.
- [18] M. Diakonou et al, Phys Lett **B89**, 432 (1980)
- [19] L. Apanasevich, FERMILAB-Pub-00/054-E (2000)
- [20] M. Acciarri et al., (L3 Collaboration) Phys. Lett. **B393**, 465-476 (1997)
- [21] R. Barate et al., (ALEPH Collaboration) Phys. Rep. **294**, 1-165 (1998)
- [22] K. Ackerstaff et al., (OPAL Collaboration) Eur. Phys. Jour. **C5**, 411-437 (1998)
- [23] X. Cai (for the STAR Collaboration) Nucl. Phys. **A774**, 485-488, (2006)
- [24] M. Naruki et al, Phys. Rev. Lett. **96**, 092301, (2006)
- [25] J. Adams et al., (STAR Collaboration) Phys. Rev. Lett. **92**, 092301, (2004)
- [26] D. Trnka et al, Phys. Rev. Lett. **94**, 192303, (2005)
- [27] Particle Data Group. S. Edelman, et.al. Phys. Lett. **B592**, 1 (2004)